Thermal Conductivity of Geometrically Frustrated, Ferroelectric $YMnO_3$: Extraordinary Spin-Phonon Interactions

P. A. Sharma,[1] J. S. Ahn,[1,2,*] N. Hur,[1] S. Park,[1] Sung Baek Kim,[1] Seongsu Lee,[2,3] J.-G. Park,[2,3] S. Guha,[1] and S-W. Cheong[1]

[1]*Department of Physics & Astronomy, Rutgers University, Piscataway, New Jersey 08854 USA*
[2]*CSCMR, Seoul National University, Seoul 405-751, Korea*
[3]*Department of Physics & Institute of Basic Science, SungKyunKwan University, Suwon 440-746, Korea*

(Received 6 June 2003; published 20 October 2004)

The thermal conductivity of the magnetically frustrated, ferroelectric $YMnO_3$ exhibits an isotropic suppression in the cooperative paramagnetic state, followed by a sudden increase upon magnetic ordering. This unprecedented behavior without an associated *static* structural distortion probably originates from the strong dynamic coupling between acoustic phonons and low-energy spin fluctuations in geometrically frustrated magnets. The replacement of magnetic Ho for Y at the ferroelectrically active site results in an even larger effect, suggestive of the strong influence of multiferroicity.

DOI: 10.1103/PhysRevLett.93.177202 PACS numbers: 75.40.–s, 66.70.+f, 75.47.Lx, 75.80.+q

A multiferroic is a material that possesses both ferroelectricity and magnetism. These properties are thought to be nearly mutually exclusive. In fact, multiferroics are a very rare occurrence [1]. Hexagonal $YMnO_3$ is one of the most well-known examples of multiferroics. The ferroelectric (FE) transition occurs above 900 K, and antiferromagnetic (AF) order has been observed at ~70–80 K. Mn^{3+} ($S = 2$) spins interact antiferromagnetically within the hexagonal layers of the structure, indicating that the magnetism is geometrically *frustrated* (GF). Thus, $YMnO_3$ is a unique GF multiferroic. The coexistence of novel magnetism and ferroelectricity is suggestive of a peculiar interaction between the spin and lattice degrees of freedom, the understanding of which remains an open problem.

The possibility of coupling between magnetic and FE order has stimulated a renewed interest in the hexagonal manganites. While various crystallographic, optical, and magnetic structural studies have been performed to independently understand the FE and magnetic properties [2–4], less progress has been made to understand their interrelation. Some hint for this coupling has been found through measurements of the dielectric constant [5], which has been confirmed on $YMnO_3$ single crystals [6]. Nonlinear optical and reflectance measurements have revealed more detailed information about the spin-lattice interaction, yet the strength of this interaction remains uncertain [7,8]. Because of the unusual sensitivity of GF materials to slight perturbations [9], the coupling between GF magnetism and ferroelectricity could be dramatically enhanced.

We have discovered striking evidence for dynamic spin-lattice coupling in $YMnO_3$ through measurements of the thermal conductivity (κ). Our results show a large increase in κ both in the ab plane and along the c direction of $YMnO_3$ below the Néel temperature T_N which we have associated with the decrease of acoustic phonon scattering by low-energy spin fluctuations. Identical experiments on $HoMnO_3$, for which the nonmagnetic Y^{3+} ion is replaced with magnetic Ho^{3+} at the ferroelectrically active crystallographic site, show an even larger suppression of κ in a much wider T range, further suggesting the influence of ferroelectricity.

Single crystalline $YMnO_3$ was grown using the floating zone method, and polycrystalline specimens were synthesized using the standard solid-state reaction. $\kappa(T)$ was measured using the steady state method and heat capacity $C(T)$ was measured using a relaxational method in a Quantum Design Physical Property Measurement System from 2–300 K. Magnetic susceptibility (χ) was measured using a Quantum Design SQUID magnetometer in a field of 2 kOe. The dielectric constant ε was measured using an *LCR* meter at a frequency of 1 kHz with an excitation of 1 V.

$\kappa(T)$ displayed in the upper panel of Fig. 1 is directly compared with χ and C in the bottom panel. The correlation between the thermal and magnetic properties is evident. At high T, κ in the ab plane and the c direction shows a relatively weak T dependence. $\kappa(T)$ drops gradually as T is lowered but then undergoes a sharp increase at the onset of AF order ($T_N \approx 75$ K), in direct correlation with features in χ and C. A second transition in χ was observed at 40 K (likely a Mn spin reorientation), but had no reproducible connection to any $\kappa(T)$ feature. Upon application of magnetic field, $H = 90$ kOe [displayed as κ(0 kOe)–κ(90 kOe) with open symbols in Fig. 1], the high-T κ remained the same, while at low T, a small H-induced suppression was observed that was slightly larger for κ_c relative to κ_{ab}. Evidently, the magnitude of κ above T_N is considerably suppressed. The Curie-Weiss temperature Θ_{CW}, inferred from $1/\chi$, was approximately 650 K so that $\Theta_{CW}/T_N \sim 8.7$, demonstrating the presence of geometrical frustration [6]. In GF magnets, strongly interacting spins fluctuate cooperatively for

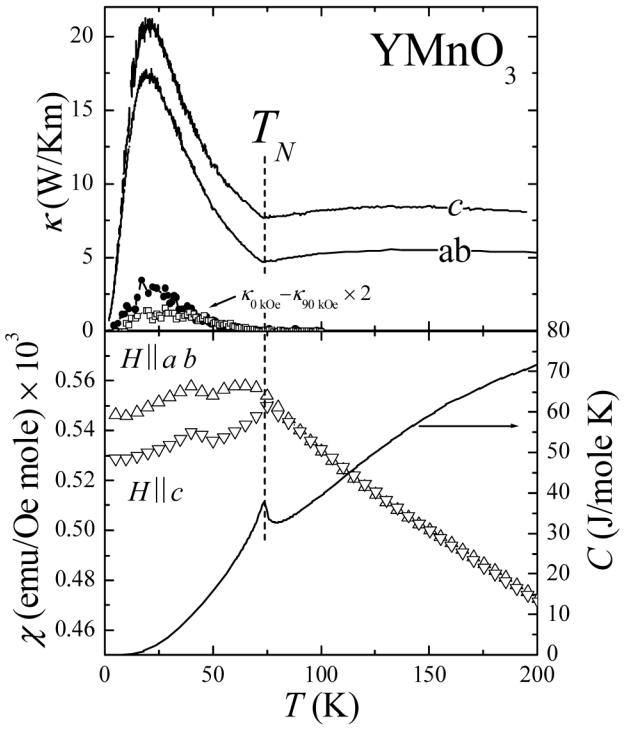

FIG. 1. .Upper panel: $\kappa(T)$ measured for the different crystal directions in single crystal $YMnO_3$ at 0 kOe. The symbols represent the difference: $\kappa_{0\ \mathrm{kOe}} - \kappa_{90\ \mathrm{kOe}}$ along the ab plane (open squares) and the c axis (filled circles) and show the negligible H dependence of this effect. Lower panel: $\chi(T)$ measured at 2 kOe for the different crystal directions. $C(T)$ measured at 0 kOe. The observed sharp feature in κ at T_N is coincident with features in χ and C.

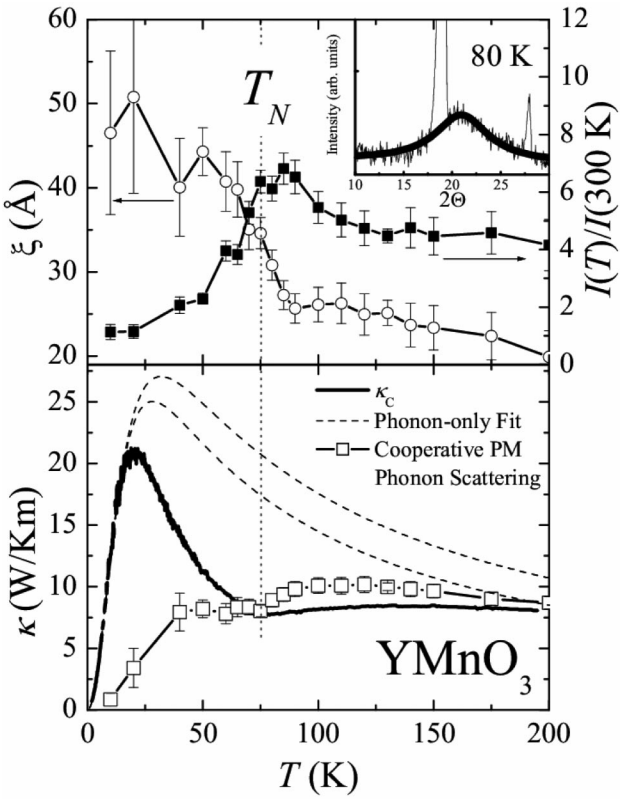

FIG. 2. .Upper panel: Magnetic correlation length $\xi(T)$ determined from diffuse scattering observed in the neutron powder diffraction. Inset: Typical data set at 80 K showing the diffusive scattering peak along with the sharp nuclear Bragg peaks. Lower panel: The solid line indicates the measured $\kappa_c(T)$ of $YMnO_3$. The dashed lines represent two separate fits to κ_c, assuming only phonon interactions. The open squares represent our model for the effect of spin fluctuations on κ. The agreement of this model with the data is successful above T_N. For $T < T_N$, this model is not expected to be valid.

$T_N < T < \Theta_{\mathrm{CW}}$ due to the enormous ground state degeneracy [10]. As discussed later, heat is carried solely by acoustic phonons in this material, which are in turn strongly coupled with these spin fluctuations.

We were able to model the effect on κ due to spin fluctuations present above T_N in $YMnO_3$ using diffusive neutron scattering measurements [11,12]. Such experiments yield an estimate for the appearance of "static" (on the time scale of $\sim 10^{-11}$ sec) short-range order (SRO) and confirm the presence of low-energy spin fluctuations well above T_N. The upper panel of Fig. 2 displays the magnetic correlation length $\xi(T)$ and normalized intensity $I(T)/I(300\ \mathrm{K})$ determined from the width and the area of the diffuse scattering peaks, respectively [11]. The analysis results are presented in the bottom panel of Fig. 2. First, the Debye-Calloway model for the lattice κ was fit to our experimental data, shown as dashed and solid lines, respectively [13]. For clarity, only the fit for κ_c is shown, but similar results were also obtained for κ_{ab}. In this model, we accounted for the effects of dislocations, point defect, phonon-phonon, and boundary scattering [14]. This model fits our data well at low T, but clearly fails at high T [15]. From kinetic theory, the phonon scattering rate is of the form $n_0 v_s \sigma$, where σ is the scattering cross section, v_s is the speed of sound, and n_0 is the density of scatterers [16]. As a simplified model for phonon scattering by spin fluctuations, we let $\sigma = \pi(\xi/2)^2$: spherical objects of average size ξ present a σ independent of phonon wavelength λ_p. This geometrical approximation is only valid in the short wavelength limit $\lambda_p \ll \xi$ [17]. The scatterer density was given by $n_0 = N[I(T)/I(300\ \mathrm{K})]$, where N is the only adjustable constant. The expression $N[I(T)/I(300\ \mathrm{K})]v_s\pi(\xi/2)^2$ was combined with the phonon scattering rates of the previous phonon fit.

The inclusion of this magnetic scattering rate is displayed as solid symbols in the lower panel of Fig. 2. The prefactor N was adjusted to fit the observed magnitude of $\kappa(75\ \mathrm{K})$; the entire magnetic scattering T dependence was assumed to originate from $\xi(T)$ and $I(T)$. Despite the simplicity of this model, the κ data have been reproduced well. Below T_N, this model fails, since the approximation breaks down as λ_p increases and as long range order sets in. N was found to be $\sim 0.6 \times 10^{24}\ \mathrm{m}^{-3}$, corresponding to a mean spacing between magnetic scattering centers of

~118 Å at 75 K, consistently larger than the measured $\xi(75\text{ K}) \sim 35$ Å. The mean free path, $l \approx (n_0\sigma)^{-1}$, inferred from this fit was ~417 Å at 75 K. This model indicates that *magnetic* objects of size ξ act like phonon scattering centers, probably then associated with an inhomogeneous *strain* field to incident lattice waves. These magnetic objects correspond to short-range, slowly fluctuating spin correlations associated with the spin liquid state.

In order to explore a possible connection between our observations and ferroelectricity, we have repeated our κ measurements for isostructural $HoMnO_3$. Replacing the nonmagnetic Y^{3+} ion with Ho^{3+} ($S = 2, L = 6, J = 8$) on this *ferroelectrically active* site might lead to a further κ suppression. The upper panel of Fig. 3 shows κ_{ab} and κ_c for $HoMnO_3$ as compared to $YMnO_3$. At high T, $HoMnO_3$ shows a similar weak T dependence, and overall lower magnitude as compared with $YMnO_3$. As for $YMnO_3$, κ_c shows a higher overall magnitude than κ_{ab}. Below T_N, indicated by $C(T)$ measurements, κ for both crystallographic directions shows a much smaller increase and is further suppressed for $HoMnO_3$ compared to $YMnO_3$. The sharp features in κ and C at ~72 K and ~5 K correspond to Mn and Ho AF ordering [18,19]. An increase in κ is observed along both crystal directions upon Ho spin ordering. These features are also coincident with anomalies in ε as for $YMnO_3$ at T_N [5,6,19] that might correspond to changes in the FE polarization. This is indicative of an interesting coupling between magnetism and ferroelectricity [19,20]. Intriguingly, there is an additional feature in C and ε between the T_N of Mn and Ho. This is likely a Mn spin reorientation, however, there is no associated change in κ at this transition. Our results are suggestive of a deeper connection with multiferroicity to the behavior we have observed.

Finally, we present, in Fig. 4, κ and χ measurements on two well-known isostructural variants of $YMnO_3$: $LuMnO_3$ and $ScMnO_3$ [4,6,21]. All show the coexistence of ferroelectricity and frustrated magnetism. As evident in Fig. 4, κ of polycrystalline Y, Lu, and $ScMnO_3$ increase anomalously at T_N in correlation with χ. However, this feature is greatly smeared out. This smeared behavior and the rather low absolute magnitude of κ probably result from a finite grain size, grain boundaries, or poor crystallinity. That this behavior can be seen in polycrystals greatly facilitates the study of this phenomenon in materials where crystal growth may be difficult or impossible.

The behavior of the κ we have observed in $YMnO_3$ is fascinating and utterly different from that of conventional magnetic/nonmagnetic insulators. Several possible scenarios can be ruled out for the large κ suppression at $T > T_N$. High-resolution neutron diffraction measurements have discounted the effect of any type of *static*

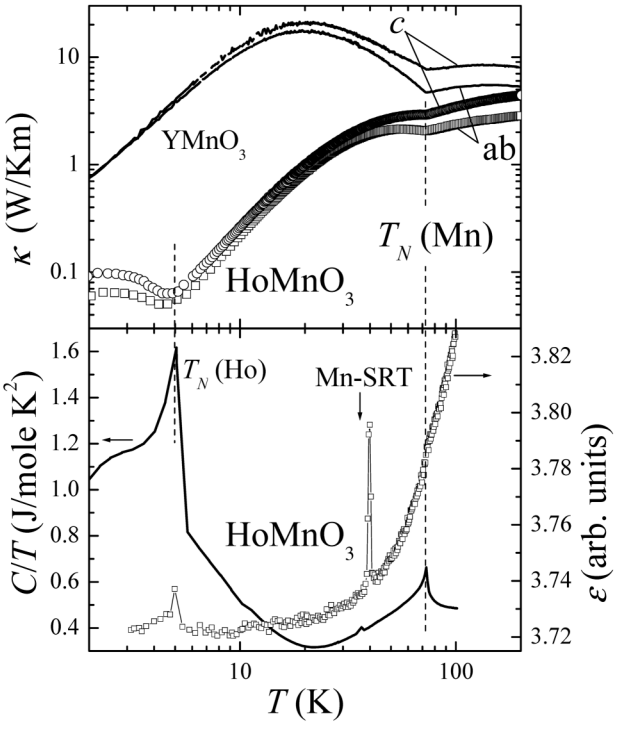

FIG. 3. .Upper panel: Open symbols represent $\kappa(T)$ for $HoMnO_3$ along the *ab* plane and the *c* axis. Substituting magnetic Ho^{3+} for nonmagnetic Y^{3+} on the ferroelectrically active crystal site results in a κ suppression over a much wider T range compared to $YMnO_3$ (solid lines). Lower panel: Features in κ are coincident with those in C/T (solid line) and the dielectric constant $\varepsilon(T)$, at T_N for Mn and Ho.

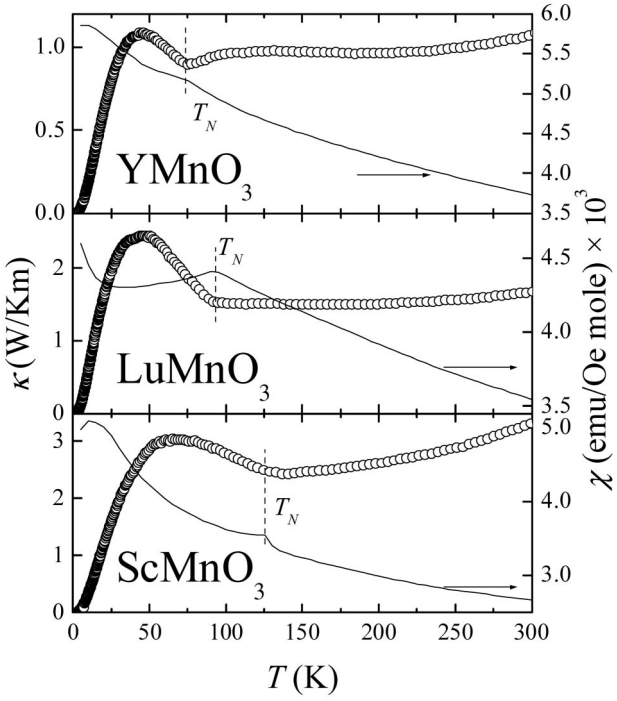

FIG. 4. .$\kappa(T)$ and $\chi(T)$ of three different isostructural multiferroic hexagonal manganites. Each polycrystalline sample shows a strikingly similar enhancement in the thermal conductivity below T_N.

structural anomalies near or at T_N [4]. Inelastic neutron scattering experiments have also shown $YMnO_3$ to be magnetically quasi-two-dimensional [22], so that any 2D magnon κ must be anisotropic in this material, while our measurements show that both κ_{ab} and κ_c undergo the same sharp rise at T_N.

The origin of a strong *dynamic* scattering mechanism of acoustic phonons may be understood as a consequence of GF. In the regime $T_N < T < \Theta_{CW}$, the strongly interacting spin system fluctuates between energetically equivalent configurations within the ground state manifold that become suppressed upon 3D ordering. If the spin system can couple to phonons, e.g., through exchange striction, then this scenario may be considered as an extreme form of critical spin scattering of phonons near a magnetic transition [23]. Such a critical scattering effect is seen in simple antiferromagnets in a very narrow T window near T_N [23,24]. Our measurements show a κ suppression in a very wide T region, up to at least 300 K, followed by a large increase below T_N where fluctuations start to disappear. Our simplified model suggests that spin-correlated regions in the high-T dynamic spin liquid state lead to a nanoscale inhomogeneous strain that scatter acoustic phonons.

These considerations suggest an unusual character of the spin-phonon interaction that may be associated with multiferroicity. An appreciable scattering of acoustic phonons by spin fluctuations may be generic in geometrically frustrated magnets [25]; however, the simultaneous presence of ferroelectricity could have important consequences for the spin-lattice interaction.

We thank J. Park for useful discussions and C. H. Lee for help during experiments at the Korean Advanced Energy Research Institute. This work was supported by NSF Grant No. DMR-0405682. J. S. A. was primarily supported by KOSEF through the CSCMR, Seoul Nat'l University. S. B. K. was partially supported by KOSEF. Work at SungKyunKwan University was supported by the CSCMR.

*Current Address: Department of Physics, Pusan National University, Pusan 609-735, Korea

[1] N. A. Hill, J. Phys. Chem. B **104**, 6694 (2000).
[2] H. L. Yakel and W. C. Koehler, Acta Crystallogr. **16**, 957 (1963).
[3] M. N. Iliev *et al.*, Phys. Rev. B **56**, 2488 (1997).
[4] A. Muñoz *et al.*, Phys. Rev. B **62**, 9498 (2000).
[5] Z. J. Huang *et al.*, Phys. Rev. B **56**, 2623 (1997).
[6] T. Katsufuji *et al.*, Phys. Rev. B **66**, 134434 (2002).
[7] M. Fiebig *et al.*, Nature (London) **419**, 818 (2002).
[8] A. B. Souchkov *et al.*, Phys. Rev. Lett. **91**, 027203 (2003).
[9] A. J. Millis, Solid State Commun. **126**, 3 (2003).
[10] R. Moessner and J. T. Chalker, Phys. Rev. Lett. **80**, 2929 (1998).
[11] Junghwan Park *et al.*, Phys. Rev. B **68**, 104426 (2003).
[12] Neutron powder diffraction experiments were carried out on polycrystalline $YMnO_3$ from ten to 300 K with $\lambda = 1.834$ Å at the high-resolution powder diffractometer of the Korean Advanced Energy Research Institute. A sample raw data set (at 80 K) is shown in the inset of the upper panel of Fig. 22. Further details may be found in Ref. [11]. A strong diffuse scattering feature appears apart from the nuclear and magnetic Bragg peaks. The nuclear and Bragg peaks were removed from the raw data. A Lorentzian function was fit to the background in order to extract the intensity and ξ at each T.
[13] See, e.g., A. V. Sologubenko *et al.*, Phys. Rev. Lett. **84**, 2714 (2000).
[14] R. Berman, *Thermal Conduction in Solids* (Clarendon, Oxford, 1976).
[15] The following scattering rates, τ_l^{-1}, were included in the Debye-Calloway model calculation: $A_1\omega$, $A_2\omega^4$, $A_3 T\omega^2 \exp[-\Theta_D/bkT]$, and v_s/L (Ref. [14]). These represent the effects of dislocations, point defects, phonon-phonon scattering, and boundary scattering, respectively. $A_1(= 20 \times 10^{-5})$, $A_2(= 1 \times 10^{-43}\mathrm{s}^3)$, and $L(= 0.2$ mm) were adjustable parameters that were chosen to reproduce the low T behavior of κ. $A_3(= 4.18 \times 10^{-18}$ s K$^{-1})$ was adjusted to account for the magnitude of κ at 300 K and should be considered rather arbitrary. For comparison, an additional fit to the data at 200 K ($A_3 = 5.76 \times 10^{-18}$ s K^{-1}) was performed; however, 4.18×10^{-18} s K^{-1} was used in all subsequent analysis. The sound velocity $v_s(= 2250$ m/s) reported by M. Chandra Sekhar *et al.*, [Mod. Phys. Lett. B **17**, 1119 (2003)] was used in the boundary scattering rate and for the calculation of $\Theta_D(= 290$ K). The parameter L was comparable with the smallest sample dimension (~ 1 mm). The value of A_1 is consistent with a dislocation density of 5×10^{10} cm^{-2}. The magnitude of A_2 is comparable to that found in similarly prepared crystals (e.g., in Ref. [13], $A_2 \sim 20$–136×10^{-43} s^3). The parameter b is given roughly as $\sim 2N^{1/3} = 6.21$, where $N(= 30)$ is the number of atoms in the unit cell, and was held fixed for the calculation.
[16] See, e.g., J. W. Schwartz and C. T. Walker, Phys. Rev. **155**, 969 (1967).
[17] In the T regime, $\lambda_p(100\ \mathrm{K}) \sim 2$–$5$ Å (Ref. [13]), about 4–10 times less than $\xi(100$ K).
[18] A. Munoz *et al.*, Chem. Mater. **13**, 1497 (2001).
[19] B. Lorenz, A. P. Litvinchuk, M. M. Gospodinov, and C. W. Chu, Phys. Rev. Lett. **92**, 087204 (2004).
[20] J. F. Scott, Rep. Prog. Phys. **12**, 1056 (1979).
[21] D. G. Tomuta *et al.*, J. Phys. Condens. Matter **13**, 4543 (2001); M. Fiebig *et al.*, Phys. Rev. Lett. **84**, 5620 (2000).
[22] T. J. Sato *et al.*, Phys. Rev. B **68**, 014432 (2003).
[23] K. Kawasaki, Prog. Theor. Phys.. **29**, 801 (1963); H. Stern, J. Phys. Chem. Solids **26**, 153 (1965).
[24] F. B. Lewis and N. H. Saunders, J. Phys. C Solid State Phys. **6**, 2525 (1973).
[25] The only other study of κ for a GF magnet was for GGG, Y. K. Tsui *et al.*, Phys. Rev. Lett. **82**, 3532 (1999). Here, $\Theta_{CW}(\sim -2$ K) is so low that the number of phonons in the spin liquid state is very small, likely making the observed effect undetectable.